

THE MASS, MORPHOLOGY, AND INTERNAL STRUCTURES OF THREE PARTICLES FROM THE HAYABUSA SAMPLE RETURN MISSION, ANALYZED WITH SYNCHROTRON RADIATION X-RAY TOMOGRAPHIC MICROSCOPY. M. M. M. Meier¹, C. Alwmark¹, S. Bajt², U. Böttger³, H. Busemann⁴, J. Gilmour⁴, U. Heitmann⁵, H.-W. Hübers³, F. Marone⁶, S. Pavlov³, U. Schade⁷, N. Spring⁴, M. Stampanoni^{6,8}, I. Weber⁵. ¹Dept. of Geology, Lund University, Sölvegatan 12, 22362 Lund, Sweden (matthias.meier@geol.lu.se), ²Photon Sci./DESY, Hamburg, Germany, ³DLR, Planet. Res. Inst., Berlin, Germany, ⁴SEAES, Univ. of Manchester, UK, ⁵Inst. f. Planetologie, Univ. of Münster, Germany, ⁶Swiss Light Source, Paul Scherrer Inst., Villigen, Switzerland, ⁷Helmholtz-Zentr., Berlin, Germany, ⁸Inst. for Biomed. Eng., Univ. & ETH Zürich, Switzerland.

Introduction: The Hayabusa sample return mission, launched in 2003 by the Japan Aerospace Exploration Agency (JAXA), was the first ever space mission to sample material from an asteroid: the S-type, near-Earth asteroid (25143) Itokawa. More than 1500 particles, varying in size from <1 μm to 180 μm , were recovered from the uppermost regolith layer of the asteroid [1-3]. The main aim of this study is to determine a precise mass for three of these particles. The mass will then be used in a forthcoming study where the concentration of solar wind-derived, trapped, and cosmogenic noble gases of the individual particles will be measured [4]. Due to the small particle size (75-145 μm), a normal weighing procedure on a micro-balance would result in large errors (up to 100%) in the mass and thus also in the noble gas concentrations, as well as the cosmic-ray-exposure (CRE) ages derived from cosmogenic noble gases. A precise mass, combined with the detection limit of the noble gas spectrometer used, allows the determination of the minimum cosmic-ray-exposure age that could still be resolved. The mass is measured by determining the volume of the constituent mineral phases (with known densities), using synchrotron radiation X-ray tomographic microscopy (SRXTM). This also allows non-destructive studies of the morphology and internal structure of the particles. While Hayabusa particles have been studied with SRXTM before [5], none of the particles from this study have so far been analyzed.

Samples & Methods: Three particles from the Hayabusa sample return mission were analyzed in this study: RA-QD02-0035, RA-QD02-0049-01 and RA-QD02-0049-04, subsequently called 35, 49-1 and 49-4. The latter two are fragments of the largest particle (orig. diam. 180 μm) from Hayabusa so far analyzed.

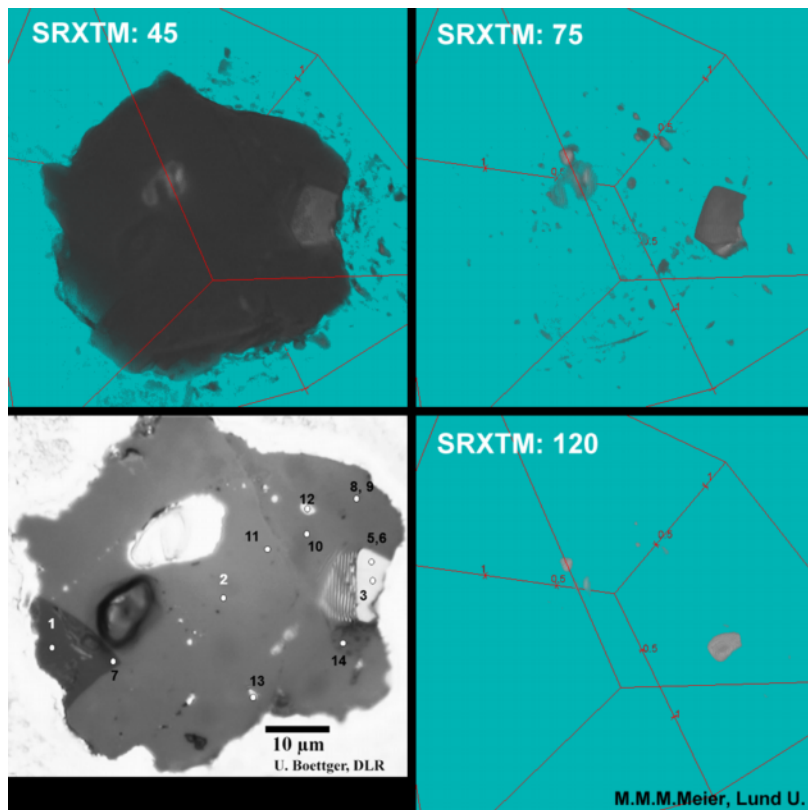


Figure 1: Comparison of SRXTM images (turquoise background) with microscope image (lower left). The view is orthogonal onto the polished surface of particle 35. Gray-scale threshold increases from top left (45; all phases visible) clockwise to lower right (120; only metal grains visible), progressively hiding mineral phases with low X-ray-attenuation coefficients. A unit distance on the grid in the SRXTM image corresponds to a length of 50 μm .

The particle has been neutron-activated [6], and these two fragments will therefore not be used for cosmogenic noble gas analysis. Particle 35 is a space-weathered grain with subsurface Fe,S nanospherules [7] and has been analyzed with SIMS for O isotopes [8]. Each of the three particles was mounted separately on a 300 μm diameter, PVDF fluorocarbon thread using a commercial, heptane-dissolvable spray-on glue. The thread was inserted in a capillary made of low-X-ray-absorbing borate glass with 700 μm inner diameter, and analyzed using SRXTM at the TOMCAT beam-line of the Swiss Light Source at the Paul Scherrer Institute,

Switzerland. Two different beam energy settings were used: 10 and 20 keV, the latter for a better resolution of mineral phases with high X-ray attenuation coefficients. The tomographic reconstructions based on the raw X-ray images were carried out on a 30-node Linux PC cluster using a gridding procedure and a highly optimized Fourier transform routine [9]. The cubic voxel size of the reconstructed images is 325 nm.

Table 1: Volumes, densities and masses

Grain	V (1000 μm^3)	ρ (g/cm 3)	M (μg)
35	72.1 \pm 2.9	3.63 \pm 0.03	0.26 \pm 0.01
49-1	444 \pm 9		1.61 \pm 0.04
49-4	96.9 \pm 1.9		0.35 \pm 0.01

Table 2: Mineral production rates

Mineral	%	ρ	P3 $_{\text{max}}$	P21 $_{\text{max}}$	P38 $_{\text{max}}$
Forsterite [MgSiO $_4$]	68- 73	3.27	1.20 (8 – 12)	0.396 (12 – 16)	0.00 N/A
Fayalite [FeSiO $_4$]	26- 31	4.39	0.866 (4 – 8)	0.0400 (8 – 12)	0.0217 (0 – 4)
Metal [Fe $_{0.95}$ Ni $_{0.05}$]	1	7	0.638 (0 – 4)	0.00917 (0 – 4)	0.0394 (0 – 4)
LL olivine	100	3.63	1.07	0.261	0.0082

Maximum production rate (in 10^{-8} ccSTP/gMa). The corresponding burial depth (in cm) in brackets.

Results & Discussion: Morphology & Internal structure: Since 49-1 and 49-4 are fragments of a larger grain, their surfaces are angular, while 35 has been polished flat on one side. All particles contain spheroid inclusions of a material with high X-ray-attenuation, probably troilite or Fe,Ni-metal (Fig. 1)[11]. **Volume & Mass determinations:** The reconstructed data sets were 3D rendered, and the volume of the different phases of each particle was calculated, using the freely available image processing program Fiji [11] and the “3D object counter” plug-in [12] for Fiji, respectively. The plug-in identifies 3D-connected objects with a gray-scale value higher than a given threshold, within an allocated image stack. While the volume will depend on the threshold, a sloped “plateau” is visible in Fig. 2. The adopted volume (Table 1) is the average of five values on the plateau (25-45), the error is the corresponding standard error (σ/\sqrt{n}). For the density, while we will eventually use the results from Raman / FTIR [4][11] once available, here we adopt the density of olivine with a Fa-number (26-31%) typical for LL chondrites, as observed by [3] for other Hayabusa olivine grains. Grains 49-1 and 49-4 have been determined to be almost monomineralic olivine [6], while for grain 35, some plagioclase and high-Ca-pyroxene is also present [7]. However, the volumetric contribution

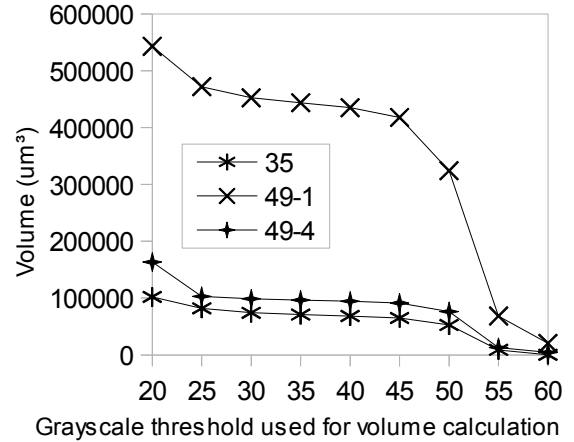


Figure 2: Volume determination for the 3 particles.

of these phases proved to be negligible (<1%). In Table 2, we list the calculated maximal mineral production rates in Fo, Fa and metal for the cosmogenic noble gas isotopes ^3He , ^{21}Ne and ^{38}Ar . All values are based on the model by [13] for an object with 500 cm radius (the largest available in that model). **Future detection of cosmogenic He, Ne:** Typical detection limits of the ultra-high sensitivity, compressor-source noble gas mass spectrometer at ETH Zurich are (in units of 10^{-15} cc-STP) 0.5 for ^3He , and 0.6 for ^{21}Ne [14]. Given the inferred masses of the three particles, and the mineral production rates in Table 2, the shortest measurable CRE ages are 0.17, 0.03, 0.13 Ma for ^3He , and 0.88, 0.14, 0.65 Ma for ^{21}Ne , from particles 35, 49-1 and 49-4 respectively. However, the biggest obstacle to a precise determination of the cosmogenic noble gas content is the presence of solar-wind-derived noble gases [15]. We are currently studying possible techniques to remove the outermost ~ 1 μm of a particle, which contains the majority of the solar-wind-implanted ions.

References: [1] Fujiwara A. et al. (2006) *Science* 312: 1330–1334. [2] Yano H. et al. (2006) *Science* 312: 1350–1353. [3] Nakamura T. et al. (2011) *Science* 333: 1113–1116. [4] Busemann H. et al. (2013), *LPS XLIV* (this meeting). [5] Tsuchiyama A. et al. (2011), *Science* 333: 1125–1128. [6] Ebihara M. et al. (2011), *Science* 333: 1119–1121. [7] Noguchi T. et al. (2011), *Science* 333: 1121–1125. [8] Yurimoto H. et al. (2011), *Science* 333: 1116–1119. [9] Marone F. & Stampanoni M. (2012), *J. Synchrotron Rad.* 19: 1029–1037. [10] Boettger U. et al. (2013), *LPS XLIV* (this meeting). [11] Schindelin J. et al. (2012), *Nature Methods* 9: 676–682. [12] Bolte S. and Cordelières F.P. (2006), *J. Microsc.* 224: 213–232. [13] Leya I. and Masarik J. (2009), *Meteorit. Planet. Sci.* 44: 1061–1086. [14] Meier M.M.M. et al. (2012), *Geochim. Cosmochim. Acta* 76: 147–160. [15] Nagao K. et al. (2011), *Science* 333: 1128–1131.